

## Electronic Supplementary Information

### A Fluidized Electrocatalysis Approach for Ammonia Synthesis Using Oxygen Vacancy-Rich Co<sub>3</sub>O<sub>4</sub> Nanoparticles

Wenyi Li,<sup>†ab</sup> Yixing Ye,<sup>†a</sup> Shengbo Zhang,<sup>a</sup> Changhao Liang,<sup>\*a</sup> and Haimin Zhang,<sup>\*a</sup>

<sup>a</sup> Key Laboratory of Materials Physics, Centre for Environmental and Energy Nanomaterials, Anhui Key Laboratory of Nanomaterials and Nanotechnology, CAS Center for Excellence in Nanoscience, Institute of Solid State Physics, HFIPS, Chinese Academy of Sciences, Hefei 230031, China. E-mail: *chliang@issp.ac.cn*, *zhanghm@issp.ac.cn*.

<sup>b</sup> University of Science and Technology of China, Hefei 230026, China.

### Supplementary Tables and Figures

**Table S1** The comparable results of our work and other recently reported NRR electrocatalysts.

Catalyst	System /Conditions	NH <sub>3</sub> Yield Rate	FE (%)	Detection method	Ref.
L-Co <sub>3</sub> O <sub>4</sub> -4.0	0.1 M Na <sub>2</sub> SO <sub>4</sub> (pH =10.5)	<b>Fluidized electrocatalysis system</b> <b>235.0 μg h<sup>-1</sup> mg<sub>cat.</sub><sup>-1</sup></b> <b>(-0.30 V vs. RHE)</b> <b>Catalyst-loading electrocatalysis system</b> <b>49.6 μg h<sup>-1</sup> mg<sup>-1</sup></b> <b>(-0.30 V vs. RHE)</b>	<b>20.7</b> <b>(-0.20 V vs. RHE)</b> <b>9.9</b> <b>(-0.20 V vs. RHE)</b>	<b>Indophenol method</b>	<b>This work</b>
NiO NDs/G	0.1 M Na <sub>2</sub> SO <sub>4</sub>	18.6 μg h <sup>-1</sup> mg <sup>-1</sup> (-0.7 V vs. RHE)	7.8	Indophenol method	1
CuO/RGO	0.1 M Na <sub>2</sub> SO <sub>4</sub>	1.8×10 <sup>-1</sup> mol s <sup>-1</sup> cm <sup>-2</sup> (-0.75 V vs. RHE)	3.9	Indophenol method	2
CoO QD/RGO	0.1 M Na <sub>2</sub> SO <sub>4</sub>	21.5 μg h <sup>-1</sup> mg <sup>-1</sup> (-0.6 V vs. RHE)	8.3	Indophenol method	3
Mo <sub>2</sub> C/C	0.5 M Li <sub>2</sub> SO <sub>4</sub> (PH =2)	11.3 μg h <sup>-1</sup> mg <sup>-1</sup> <sub>Mo<sub>2</sub>C</sub> (-0.3 V vs. RHE)	7.8	Nessler method	4
ZnO QDs/RGO	0.1 M Na <sub>2</sub> SO <sub>4</sub>	17.7 μg h <sup>-1</sup> mg <sup>-1</sup> (-0.65 V vs. RHE)	6.4	Indophenol method	5

SnO <sub>2</sub> QDs/RGO	0.1 M Na <sub>2</sub> SO <sub>4</sub>	25.6 μg h <sup>-1</sup> mg <sup>-1</sup> (-0.5 V vs. RHE)	7.1	Indophenol method	6
P-WO <sub>3</sub> @TiO <sub>2</sub>	0.1 M Na <sub>2</sub> SO <sub>4</sub>	6.54×10 <sup>-10</sup> mol s <sup>-1</sup> cm <sup>-2</sup> (-0.55 V vs. RHE)	17.5 (-0.35 V vs. RHE)	Indophenol method	7
Cr <sub>2</sub> O <sub>3</sub> nanofiber	0.1 M HCl	28.13 μg h <sup>-1</sup> mg <sup>-1</sup> (-0.75 V vs. RHE)	8.56	Indophenol method	8
Bi <sub>4</sub> O <sub>11</sub> /CeO <sub>2</sub>	0.1 M HCl (pH = 1)	23.21 μg h <sup>-1</sup> mg <sub>cat.</sub> <sup>-1</sup> (-0.2 V vs. RHE)	10.16	Indophenol method	9
Nb <sub>2</sub> O <sub>5</sub> /CP	0.1 M HCl	43.6 μg h <sup>-1</sup> mg <sub>cat.</sub> <sup>-1</sup> (-0.55 V vs. RHE)	9.26	Indophenol method	10
MXene (Ti <sub>3</sub> C <sub>2</sub> T <sub>x</sub> )	0.5 M Li <sub>2</sub> SO <sub>4</sub> + 0.1 M HCl (pH = 2)	4.72 μg h <sup>-1</sup> cm <sup>-2</sup> (-0.1 V vs. RHE)	5.78	Nessler method	11
TiO <sub>2</sub> /Ti <sub>3</sub> C <sub>2</sub> T <sub>x</sub>	0.1 M HCl	32.17 μg h <sup>-1</sup> mg <sub>cat.</sub> <sup>-1</sup> (-0.45 V vs. RHE)	16.07	Indophenol method	12
OVs-rich MoO <sub>2</sub>	0.1 M HCl	12.20 μg h <sup>-1</sup> mg <sup>-1</sup> (-0.15 V vs. RHE)	8.2	Indophenol method	13
C-Ti <sub>x</sub> O <sub>y</sub> /C	0.1 M LiClO <sub>4</sub>	14.8 μg h <sup>-1</sup> mg <sub>cat.</sub> <sup>-1</sup> (-0.4 V vs. RHE)	17.8	Indophenol method	14
Fe/Fe <sub>3</sub> O <sub>4</sub>	0.1 M PBS (pH = 7.2)	~0.19 μg cm <sup>-2</sup> h <sup>-1</sup> (~0.19 μg h <sup>-1</sup> mg <sup>-1</sup> ) (-0.3 V vs. RHE)	8.29	Indophenol method	15
Zr-TiO <sub>2</sub>	0.1 M KOH	8.90 μg h <sup>-1</sup> cm <sup>-2</sup> (8.90 μg h <sup>-1</sup> mg <sup>-1</sup> ) (-0.45 V vs. RHE)	17.3	Indophenol method	16
Cu-CeO <sub>2</sub> -3.9	0.1 M Na <sub>2</sub> SO <sub>4</sub> (pH = 6.3)	5.3×10 <sup>-10</sup> mol s <sup>-1</sup> cm <sup>-1</sup> (13.3 μg h <sup>-1</sup> mg <sup>-1</sup> ) (-0.1 V vs. RHE)	19.1	Indophenol method	17
MnO <sub>x</sub> NA/TM	0.1 M Na <sub>2</sub> SO <sub>4</sub>	1.63×10 <sup>-10</sup> mol s <sup>-1</sup> cm <sup>-2</sup> (-0.5 V vs. RHE)	11.40	Indophenol method	18
α-Fe <sub>2</sub> O <sub>3</sub> nanocubes	0.1 M KOH	35.55 μg h <sup>-1</sup> mg <sub>cat.</sub> <sup>-1</sup> (-0.5 V vs. RHE)	25.93 (0.0 V vs. RHE)	Indophenol method	19
SA-Ag/NC	0.1 M HCl	270.9 μg h <sup>-1</sup> mg <sub>cat.</sub> <sup>-1</sup> 69.4 mg h <sup>-1</sup> mg <sub>Ag</sub> <sup>-1</sup> (-0.6 V vs. RHE)	21.9 (-0.65 V vs. RHE)	Indophenol method	20
Zn/Fe-N-C	0.1 M PBS	30.5 μg h <sup>-1</sup> mg <sub>cat.</sub> <sup>-1</sup> (-0.3 V vs. RHE)	26.5	Indophenol method	21
Au <sub>1</sub> /C <sub>3</sub> N <sub>4</sub>	0.005 M H <sub>2</sub> SO <sub>4</sub>	1,305 μg h <sup>-1</sup> mg <sup>-1</sup> <sub>Au</sub> (-0.1 V vs. RHE)	11.1	Indophenol method	22
Au@amorphous SnO <sub>2</sub> NPs	0.1 mol L <sup>-1</sup> HCl	21.9 μg h <sup>-1</sup> mg <sub>cat.</sub> <sup>-1</sup> (-0.2 V vs. RHE)	15.3	Indophenol method	23

Ru@ZrO <sub>2</sub> /NC	0.1 M HCl	3.665 mg <sub>NH<sub>3</sub></sub> h <sup>-1</sup> mg <sub>Ru</sub> . <sup>-1</sup> (-0.21 V vs. RHE)	21 (-0.11 V vs. RHE)	Indophenol method	24
SA-Mo/NPC	0.1 M KOH	34.0 ± 3.6 μg <sub>NH<sub>3</sub></sub> h <sup>-1</sup> mg <sub>cat.</sub> . <sup>-1</sup> (-0.3 V vs. RHE)	14.6 ± 1.6	Nessler method	25
ISAS-Fe/NC	0.1 M PBS	62.9 ± 2.7 μg h <sup>-1</sup> mg <sub>cat.</sub> . <sup>-1</sup> (-0.4 V vs. RHE)	18.6 ± 0.8	Indophenol method	26
Bi NS	0.5 M K <sub>2</sub> SO <sub>4</sub> (pH = 3.5)	200 mmol g <sup>-1</sup> h <sup>-1</sup> 0.052 mmol cm <sup>-2</sup> h <sup>-1</sup> (3400 μg h <sup>-1</sup> mg <sup>-1</sup> )	66	Nessler method	27
FL-BP NSs	0.01M HCl	31.37 μg h <sup>-1</sup> mg <sup>-1</sup> (-0.7 V vs. RHE)	5.07 (-0.6 V vs. RHE)	Indophenol method	28
VN NPs	0.05M H <sub>2</sub> SO <sub>4</sub>	3.3 × 10 <sup>-10</sup> mol s <sup>-1</sup> cm <sup>-1</sup> (40.4 μg h <sup>-1</sup> mg <sup>-1</sup> ) (-0.1 V vs. RHE)	6.0	Nessler method	29
MBN	0.1 M Na <sub>2</sub> SO <sub>4</sub>	18.2 μg h <sup>-1</sup> mg <sub>cat.</sub> . <sup>-1</sup> (-0.7 V vs. RHE)	5.5	Indophenol method	30
PCN	0.1 M HCl	8.09 μg h <sup>-1</sup> mg <sub>cat.</sub> . <sup>-1</sup> (-0.2 V vs. RHE)	11.05	Indophenol method	31
B <sub>4</sub> C/CPE	0.1 M HCl	26.57 μg h <sup>-1</sup> mg <sub>cat.</sub> . <sup>-1</sup> (-0.75 V vs. RHE)	15.95	Indophenol method	32
TiC/C	0.1 M HCl	14.1 μg h <sup>-1</sup> mg <sub>cat.</sub> . <sup>-1</sup> (-0.5 V vs. RHE)	5.8	Indophenol method	33
ZrS <sub>2</sub> NF-Vs	0.1 M HCl	30.72 μg h <sup>-1</sup> mg <sub>cat.</sub> . <sup>-1</sup> (-0.35 V vs. RHE)	10.33 (-0.30 V vs. RHE)	Indophenol method	34
MoS <sub>2</sub>	0.1 M Na <sub>2</sub> SO <sub>4</sub>	8.08 × 10 <sup>-11</sup> mol s <sup>-1</sup> cm <sup>-1</sup> (-0.6 V vs. RHE)	1.17	Indophenol method	35
CoS <sub>2</sub> /NS-G	0.05 M H <sub>2</sub> SO <sub>4</sub>	25.0 μg h <sup>-1</sup> mg <sub>cat.</sub> . <sup>-1</sup> (-0.2 V vs. RHE)	25.9 (-0.05 V vs. RHE)	Indophenol method	36
ZrB <sub>2</sub> nanocubes	0.5 M LiClO <sub>4</sub>	37.7 μg h <sup>-1</sup> mg <sup>-1</sup> (-0.3 V vs. RHE)	18.2	Indophenol method	37
LaF <sub>3</sub>	0.5 M LiClO <sub>4</sub>	55.9 μg h <sup>-1</sup> mg <sub>cat.</sub> . <sup>-1</sup> (-0.45 V vs. RHE)	16	Indophenol method	38
Pd <sub>3</sub> Cu <sub>1</sub>	1 M KOH	39.9 mg h <sup>-1</sup> mg <sub>cat.</sub> . <sup>-1</sup> (-0.25 V vs. RHE)	1.56 (-0.05 V vs. RHE)	Nessler method	39
Rh <sub>0.6</sub> Ru <sub>0.4</sub> NAs	0.1 M Na <sub>2</sub> SO <sub>4</sub>	57.75 μg h <sup>-1</sup> mg <sub>cat.</sub> . <sup>-1</sup> (-0.2 V vs. RHE)	3.39	Indophenol method	40
PdCuIr	0.1 M Na <sub>2</sub> SO <sub>4</sub>	13.43 μg h <sup>-1</sup> mg <sub>cat.</sub> . <sup>-1</sup> (-0.3 V vs. RHE)	5.29	Indophenol method	41

amorphous BiNi alloy	0.1 M Na <sub>2</sub> SO <sub>4</sub>	17.5 μg h <sup>-1</sup> mg <sub>cat.</sub> <sup>-1</sup> (-0.6 V vs. RHE)	13.8	Indophenol method	42
NPC	0.05 M H <sub>2</sub> SO <sub>4</sub>	1.40 mmol g <sup>-1</sup> h <sup>-1</sup> (23.8 μg h <sup>-1</sup> mg <sup>-1</sup> ) (-0.9 V vs. RHE)	1.42	Nessler method	43
NPC-500	0.005 M H <sub>2</sub> SO <sub>4</sub>	1.31 mmol g <sup>-1</sup> h <sup>-1</sup> (22.3 μg h <sup>-1</sup> mg <sup>-1</sup> ) (-0.4 V vs. RHE)	9.98	Indophenol method	44
CC-450	0.1 M Na <sub>2</sub> SO <sub>4</sub> + 0.02 M H <sub>2</sub> SO <sub>4</sub>	15.8 μg cm <sup>-2</sup> h <sup>-1</sup> (-0.3 V vs. RHE)	6.92	Indophenol method	45
d-FG	0.1 M Na <sub>2</sub> SO <sub>4</sub>	9.3 μg h <sup>-1</sup> mg <sub>cat.</sub> <sup>-1</sup> (-0.7 V vs. RHE)	4.2	Indophenol method	46
Fe-N/C-CNTs	0.1 M KOH	34.83 μg h <sup>-1</sup> mg <sub>cat.</sub> <sup>-1</sup> (-0.2 V vs. RHE)	9.28	Indophenol method	47
BG	0.05 M H <sub>2</sub> SO <sub>4</sub>	9.8 μg cm <sup>-2</sup> h <sup>-1</sup> (11.0 μg h <sup>-1</sup> mg <sup>-1</sup> ) (-0.5 V vs. RHE)	10.8	Indophenol method	48
BCN	0.1 M HCl	7.75 μg h <sup>-1</sup> mg <sub>cat.</sub> <sup>-1</sup> (-0.3 V vs. RHE)	13.79	Indophenol method	49
IrP <sub>2</sub> @PNPC-NF	0.05 M H <sub>2</sub> SO <sub>4</sub>	94.0 μg h <sup>-1</sup> mg <sub>cat.</sub> <sup>-1</sup> (-0.3 V vs. RHE)	17.8 (-0.1 V vs. RHE)	Indophenol method	50

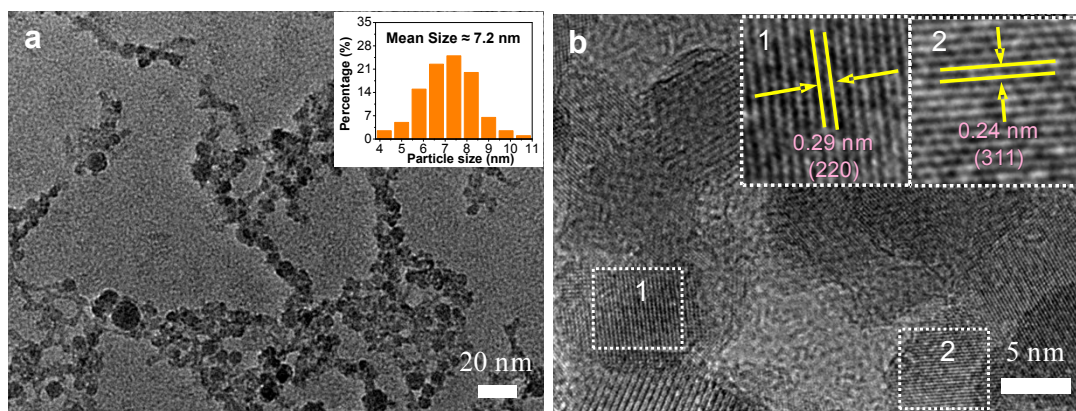


**Fig. S1** (a) Low-magnification TEM image of L-Co<sub>3</sub>O<sub>4</sub>-7.2 and corresponding size distribution curve. (b) High-resolution TEM image of L-Co<sub>3</sub>O<sub>4</sub>-7.2 (inset of an individual nanoparticle).

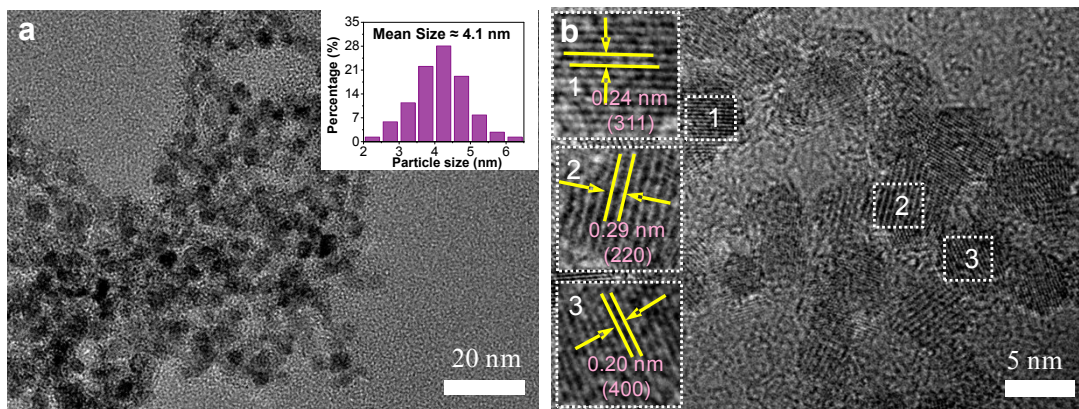


**Fig. S2** (a) Low-magnification TEM image of C-Co<sub>3</sub>O<sub>4</sub>-4.1 and corresponding size distribution curve. (b) High-resolution TEM image of C-Co<sub>3</sub>O<sub>4</sub>-4.1 (inset of an individual nanoparticle).

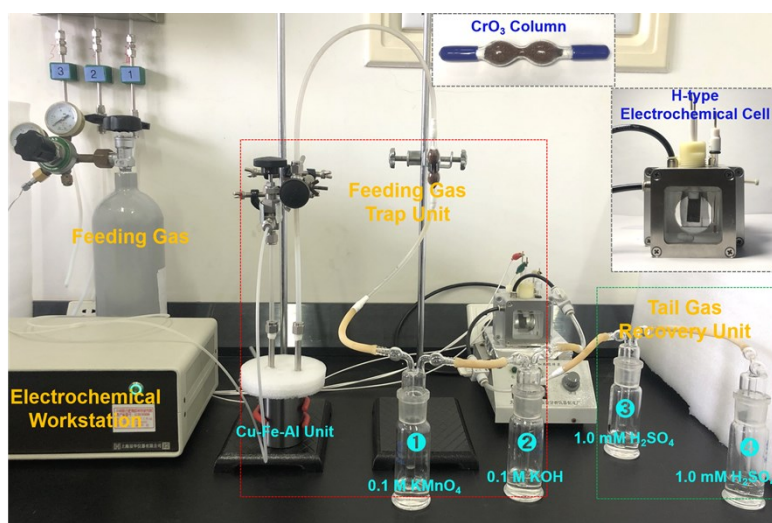


**Fig. S3** Photograph of the electrochemical NRR experimental setup.

The electrochemical NRR experimental setup was constructed to eliminate the possible interferences of  $\text{NH}_3$  and  $\text{NO}_x$  in the feeding gases based on previously reported protocol.<sup>51-53</sup> The Cu-Fe-Al catalyst (**Fig. S4**) was fabricated according to the reported methods.<sup>54-56</sup> Prior to each experiment, the Cu-Fe-Al catalyst was thermally treated at 300 °C for 2 h under 5%  $\text{H}_2/\text{Ar}$  stream. The treated Cu-Fe-Al catalyst was covered with a stainless-steel vessel which filled up with the mixed ethanol and liquid nitrogen. Moreover, a  $\text{CrO}_3$  catalyst packed column (Dongguan Zhongtian Electronic Technology Co. LTD, China) was used to completely remove NO interference. In this purification system, any NO passed through this purification unit will be converted to water soluble  $\text{NO}_2$ , and then removed by the  $\text{KMnO}_4$  and  $\text{KOH}$  before reaching the electrochemical cell.

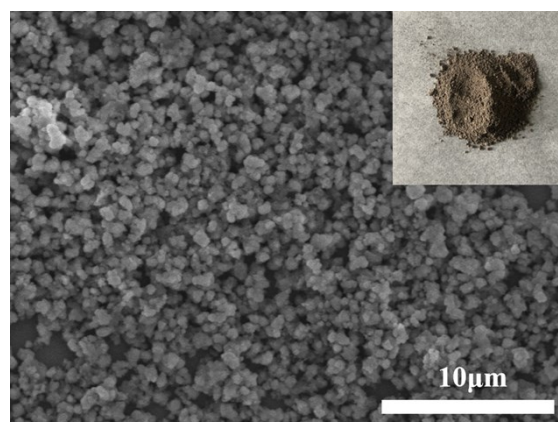


**Fig. S4** SEM image and photograph (inset) of the Cu-Fe-Al catalyst.



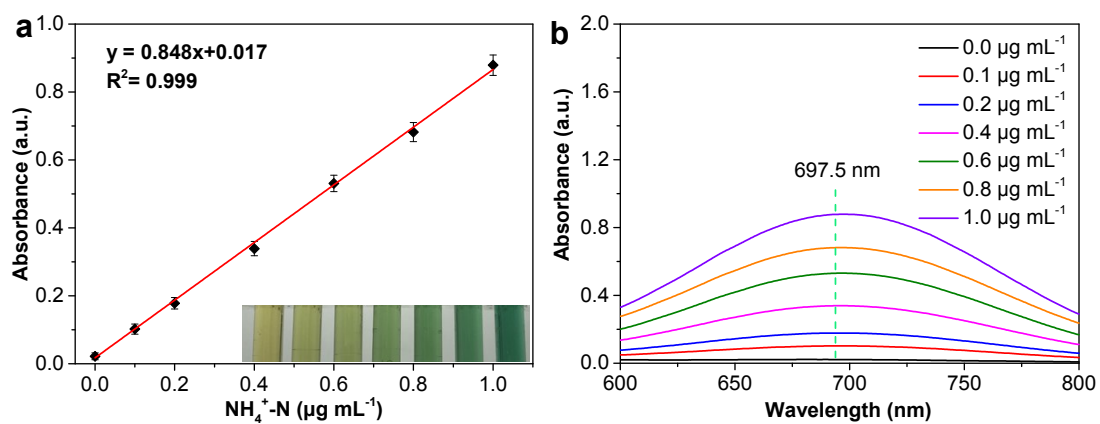


**Fig. S5** (a) The calibration curve used for calculation of  $\text{NH}_4^+\text{-N}$  concentration. (b) UV-Vis absorption spectra of the indophenol blue indicator with various concentrations of  $\text{NH}_4^+\text{-N}$  (0, 0.1, 0.2, 0.4, 0.6, 0.8, 1.0  $\mu\text{g mL}^{-1}$ ) after incubating for 1 h at room temperature.

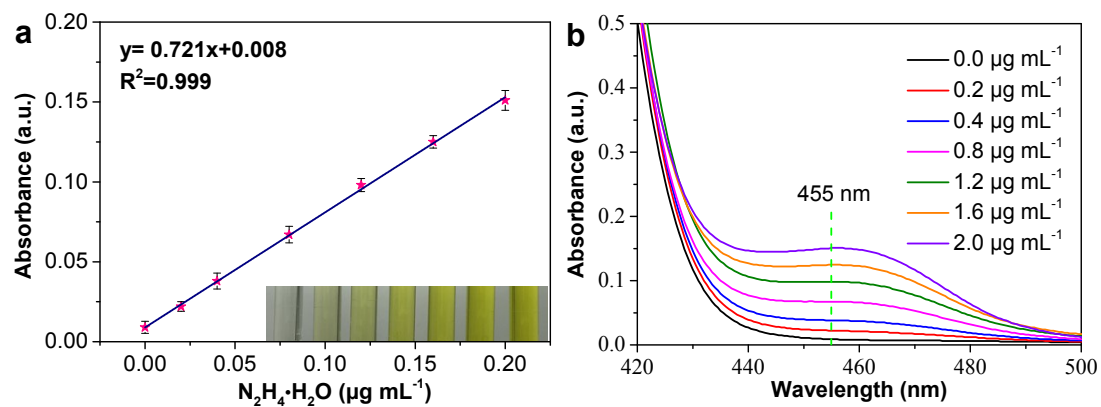


**Fig. S6** (a) The calibration curve used for calculation of  $N_2H_4 \cdot H_2O$  concentration. (b) UV-Vis absorption spectra with various concentrations of  $N_2H_4 \cdot H_2O$  (0, 0.2, 0.4, 0.8, 1.2, 1.6, 2.0  $\mu g mL^{-1}$ ) after incubating for 20 min at room temperature.

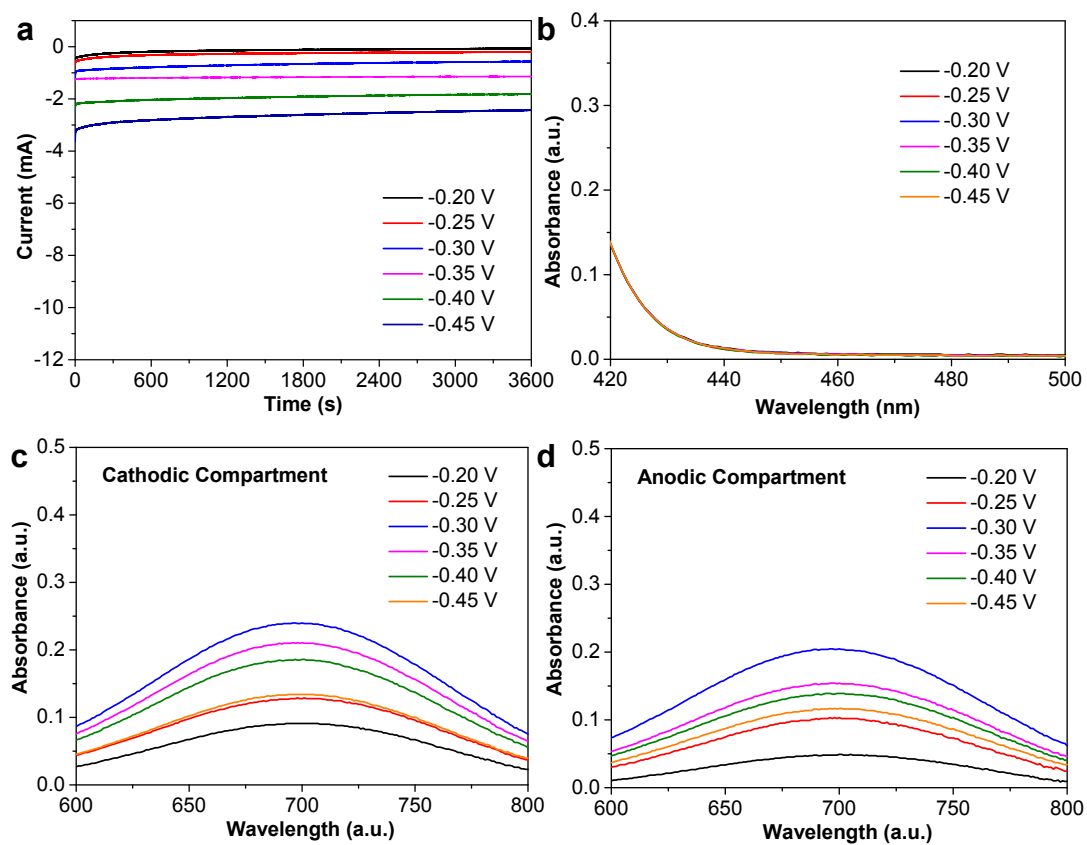


**Fig. S7** (a) Time-dependent current density curves after NRR for 1 h in  $\text{N}_2$ -saturated 0.1 M  $\text{Na}_2\text{SO}_4$  electrolyte at different potentials. UV-Vis absorption spectra of the corresponding collected samples (b) for the possible  $\text{N}_2\text{H}_4$  detection and possible  $\text{NH}_3$  detection from (c) cathodic compartment and (d) anodic compartment.

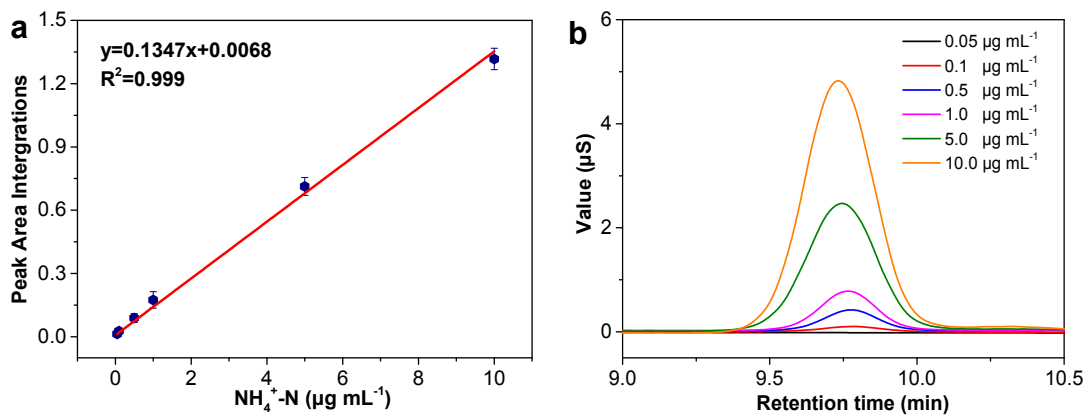


**Fig. S8** (a) The calibration curve of  $\text{NH}_4^+\text{-N}$  peak area (retention time of  $\sim 9.8$  min) used for calculation of  $\text{NH}_4^+\text{-N}$  concentration detected by the ion chromatograph. (b) The corresponding ion chromatograph spectra with various concentrations of  $\text{NH}_4^+\text{-N}$  (0.05, 0.1, 0.5, 1.0, 5.0, 10.0  $\mu\text{g mL}^{-1}$ ) in 0.1 M  $\text{Na}_2\text{SO}_4$ .

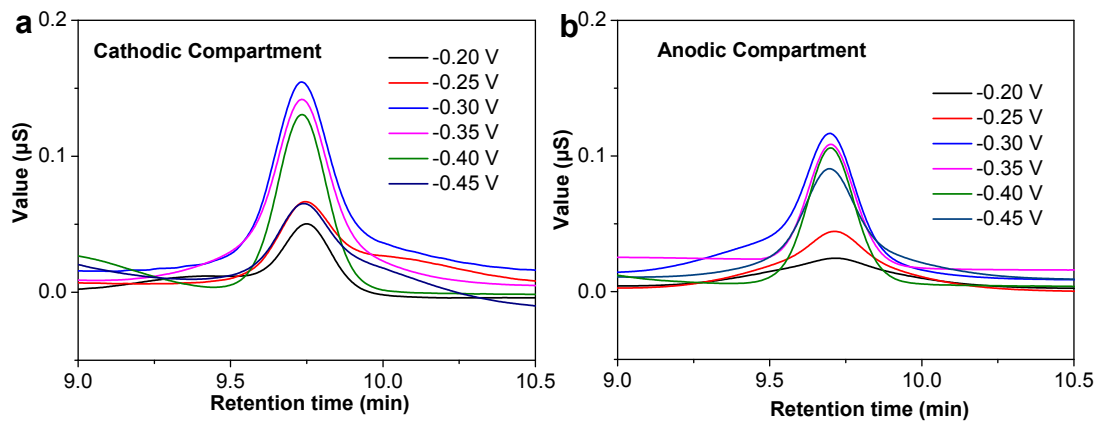


**Fig. S9** Ion chromatograph spectra of collected samples for possible  $\text{NH}_3$  detection from (a) cathodic compartment and (b) anodic compartment after NRR for 1 h in  $\text{N}_2$ -saturated 0.1 M  $\text{Na}_2\text{SO}_4$  electrolyte at different potentials.

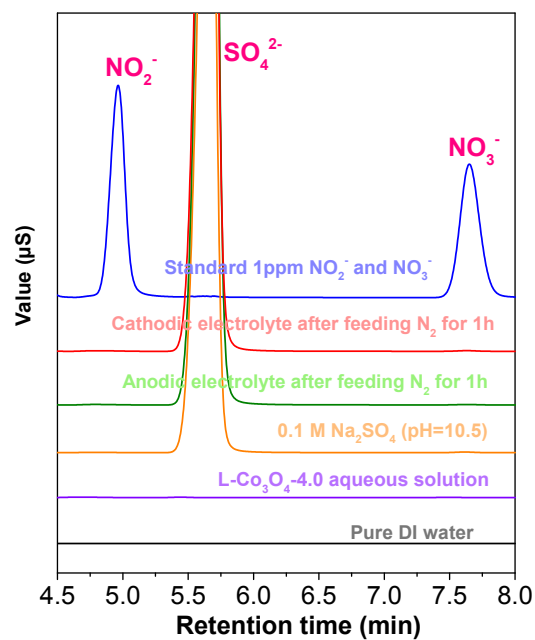


**Fig. S10** Ion chromatograph spectra of the standard solution (1.0 ppm NO<sub>2</sub><sup>-</sup> and 1.0 ppm NO<sub>3</sub><sup>-</sup>) and the collected samples under various conditions.

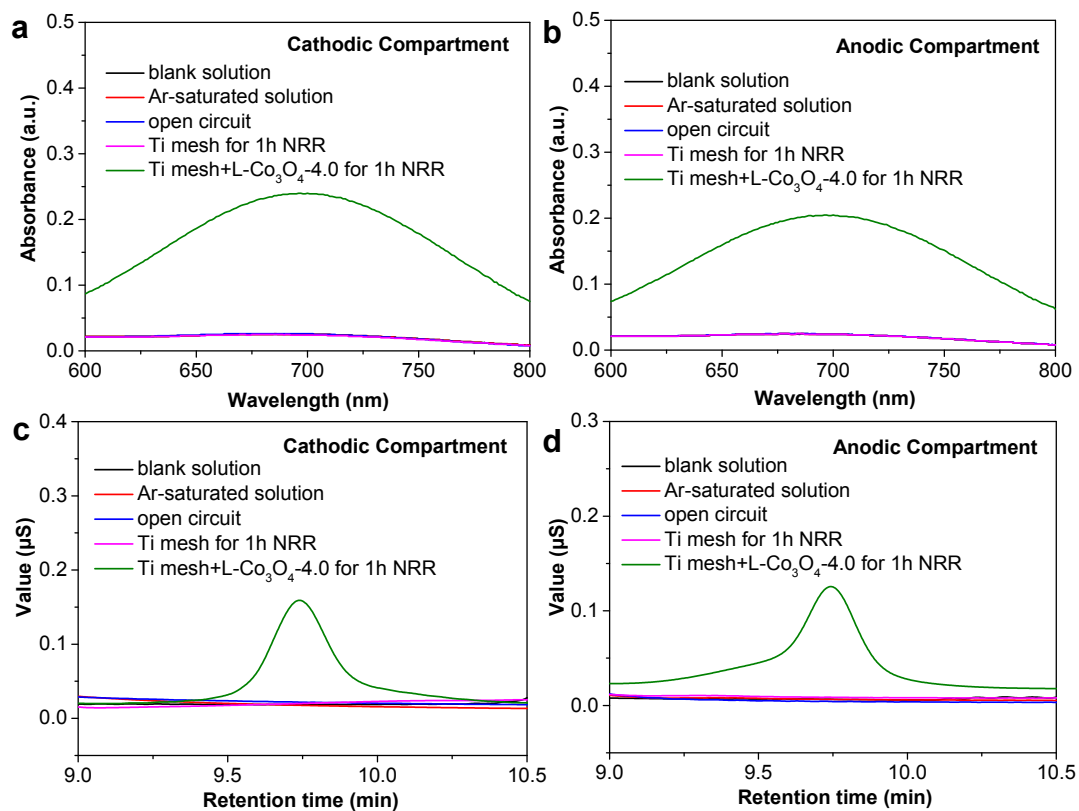


**Fig. S11** UV-Vis absorption spectra of collected solution samples from (a) cathodic compartment and (b) anodic compartment under different control conditions. Ion chromatograph spectra of collected solution samples from (c) cathodic compartment and (d) anodic compartment under different control conditions.

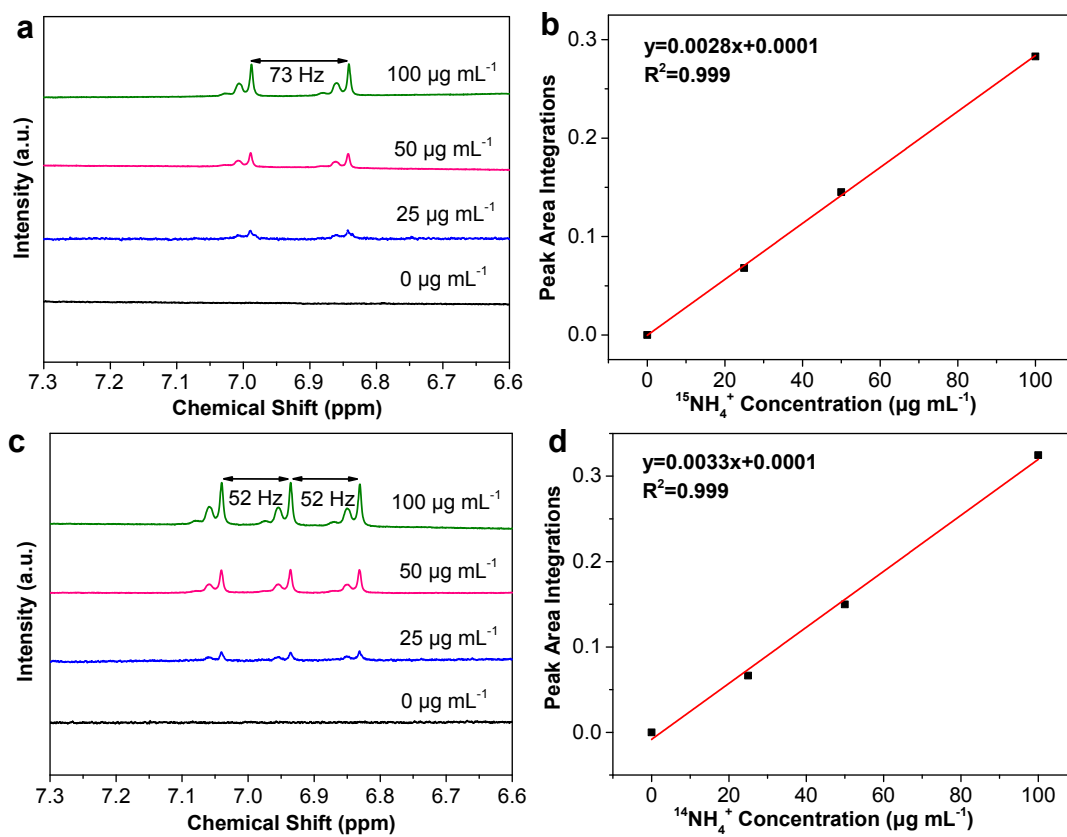


**Fig. S12** (a, c)  $^1\text{H}$  NMR spectra of the  $^{15}\text{NH}_4^+$  and  $^{14}\text{NH}_4^+$  standards with different concentrations. (b, d) Corresponding  $^{15}\text{NH}_4^+$  and  $^{14}\text{NH}_4^+$  calibration curves constructed by plotting the integrated  $^1\text{H}$  NMR signal (7.00 ppm for  $^{15}\text{NH}_4^+$  and 6.97 ppm for  $^{14}\text{NH}_4^+$ ) against the standard concentration.



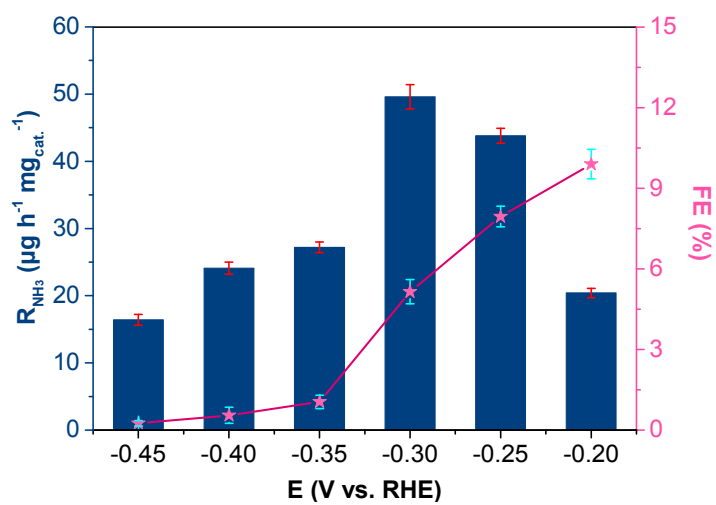


**Fig. S13** Dependence of  $R_{\text{NH}_3}$  and FE of L- $\text{Co}_3\text{O}_4$ -4.0/CC electrocatalyst at different applied potentials in  $\text{N}_2$ -saturated 0.1 M  $\text{Na}_2\text{SO}_4$  electrolyte using conventional catalyst-loading electrocatalysis system.

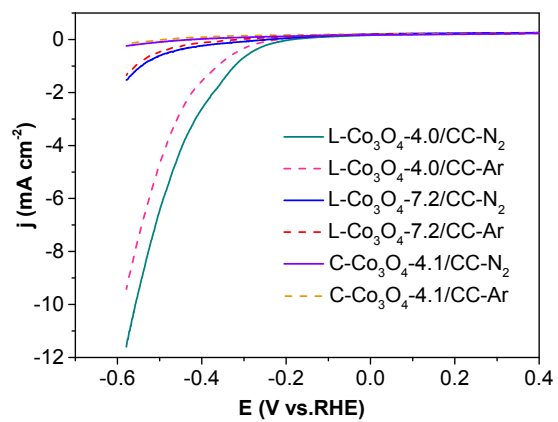


**Fig. S14** The comparison results of of LSV curves for three Co<sub>3</sub>O<sub>4</sub>/CC in N<sub>2</sub>- and Ar-saturated electrolytes.

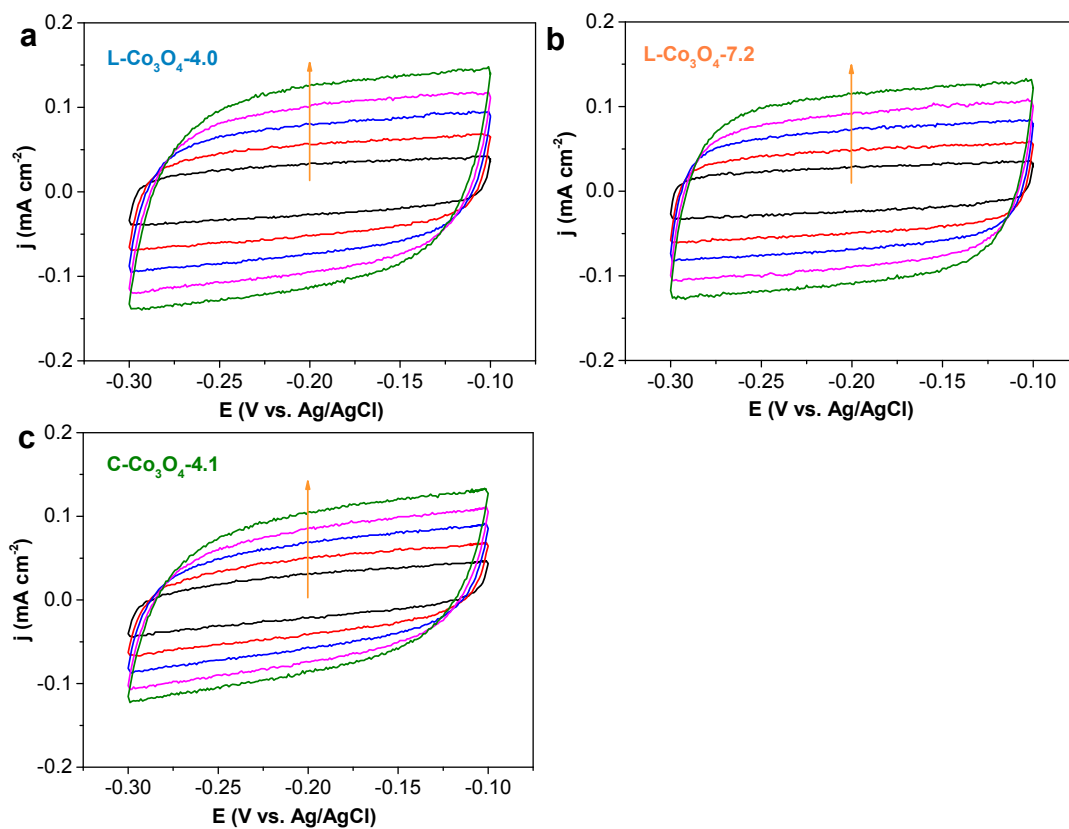


**Fig. S15** Cyclic voltammetry curves of (a)  $\text{L-Co}_3\text{O}_4-4.0$ , (b)  $\text{L-Co}_3\text{O}_4-7.2$  and (c)  $\text{C-Co}_3\text{O}_4-4.1$  with various scan rates (25, 50, 75, 100, 125  $\text{mV s}^{-1}$ ) in the region of -0.10 to -0.30 V (vs. Ag/AgCl).

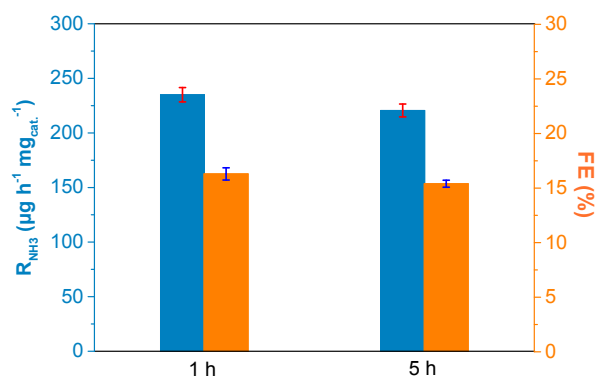


**Fig. S16** The comparison results of  $\text{NH}_3$  yield rate and FE for  $\text{L-Co}_3\text{O}_4\text{-4.0}$  in the fluidized electrocatalysis system after 1 h and 5 h of NRR, respectively.

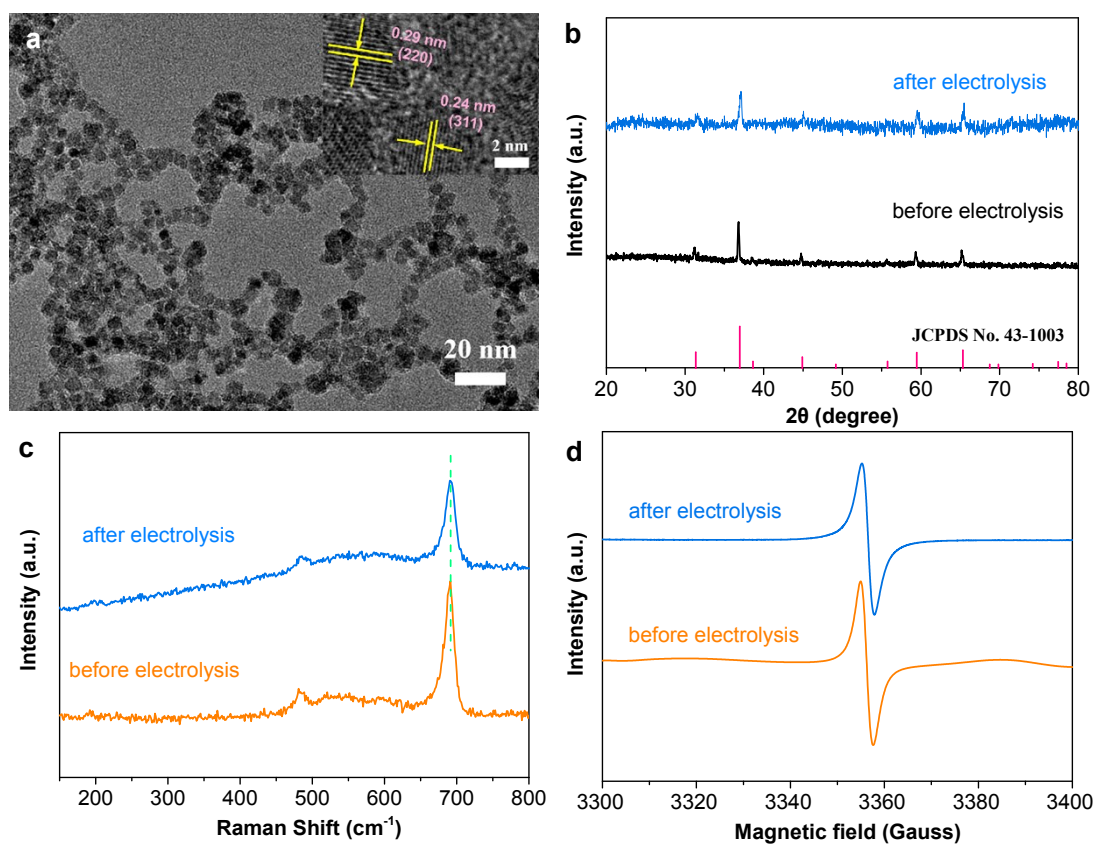


**Fig. S17** (a) TEM image and inset HRTEM image of L-Co<sub>3</sub>O<sub>4</sub>-4.0 after 5 h of NRR electrolysis. (b) XRD patterns (c) Raman spectra and (d) EPR spectra of the L-Co<sub>3</sub>O<sub>4</sub>-4.0 before and after 5 h of NRR.

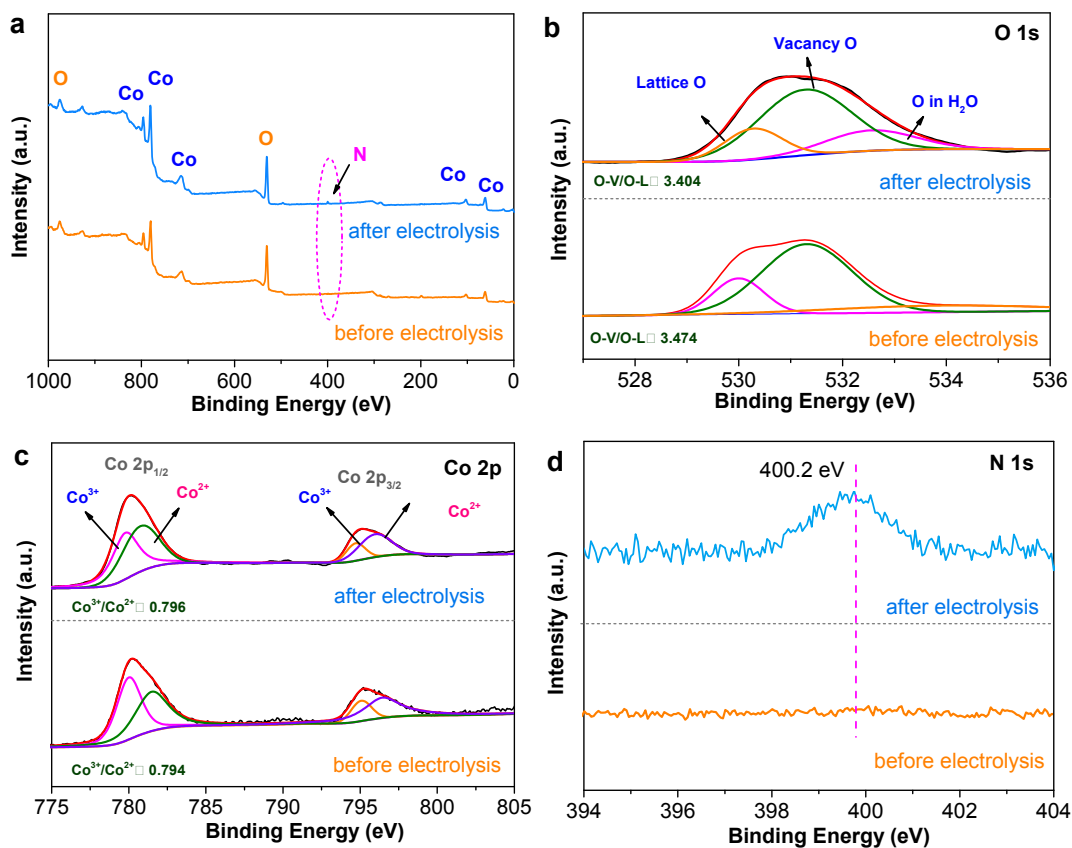


**Fig. S18** (a) The surface survey XPS spectra. (b) High-resolution O 1s XPS spectra, (c) High-resolution Co 2p XPS spectra and (d) High-resolution N 1s XPS of the L-Co<sub>3</sub>O<sub>4</sub>-4.0 before and after 5 h of NRR.

## References

1. X. H. Wang, J. Wang, Y. B. Li and K. Chu, *ChemCatChem*, 2019, **11**, 4529-4536.
2. R. Zhao, Q. Geng, L. Chang, P. Wei, Y. Luo, X. Shi, A. M. Asiri, S. Lu, Z. Wang and X. Sun, *Chem. Commun.*, 2020, **56**, 9328-9331.
3. K. Chu, Y. P. Liu, Y. B. Li, H. Zhang and Y. Tian, *J. Mater. Chem. A*, 2019, **7**, 4389-4394.
4. H. Cheng, L. X. Ding, G. F. Chen, L. Zhang, J. Xue and H. Wang, *Adv. Mater.*, 2018, **30**, 1803694.
5. Y. P. Liu, Y. B. Li, D. J. Huang, H. Zhang and K. Chu, *Chem. Eur. J.* 2019, **25**, 1 - 8.
6. K. Chu, Y. P. Liu, Y. B. Li, J. Wang and H. Zhang, *ACS Appl. Mater. Interfaces*, 2019, **11**, 4389-4394.
7. Y. Wang, J. Dai, M. Zhang, Y.-T. Liu, J. Yu and B. Ding, *Chem. Commun.*, 2020, **56**, 12937-12940.
8. H. Du, X. Guo, R.-M. Kong and F. Qu, *Chem. Commun.*, 2018, **54**, 12848-12851.
9. C. Lv, C. Yan, G. Chen, Y. Ding, J. Sun, Y. Zhou and G. Yu, *Angew. Chem., Int. Ed.*, 2018, **57**, 6073-6076.
10. J. Han, Z. Liu, Y. Ma, G. Cui, F. Xie, F. Wang, Y. Wu, S. Gao, Y. Xu and X. Sun, *Nano Energy*, 2018, **52**, 264-270.
11. Y. Luo, G. F. Chen, L. Ding, X. Chen, L. X. Ding and H. Wang, *Joule*, 2019, **3**, 279-289.
12. Y. Fang, Z. Liu, J. Han, Z. Jin, Y. Han, F. Wang, Y. Niu, Y. Wu and Y. Xu, *Adv. Energy Mater.*, 2019, **0**, 1803406.
13. G. Zhang, Q. Ji and K. Zhang, *Nano Energy*, 2019, **59**, 10-16.
14. Q. Qin, Y. Zhao, M. Schmallegger, T. Heil, J. Schmidt, R. Walczak, G. Gescheidt-Demner, H. Jiao and M. Oschatz, *Angew. Chem., Int. Ed.*, 2019, **58**, 2-8.
15. L. Hu, A. Khaniya, J. Wang, G. Chen, W. E. Kaden and X. Feng, *ACS Catal.*, 2018, **8**, 9312-9319.
16. N. Cao, Z. Chen, K. Zang, J. Xu, J. Zhong, J. Luo, X. Xu and G. Zheng, *Nat. Commun.*, 2019, **10**, 2877.
17. S. Zhang, C. Zhao, Y. Liu, W. Li, J. Wang, G. Wang, Y. Zhang, H. Zhang and H. Zhao, *Chem. Commun.*, 2019, **55**, 2952-2955.
18. L. Zhang, X. Y. Xie, H. Wang, L. Ji, Y. Zhang, H. Chen, T. Li, Y. Luo, G. Cui and X. Sun, *Chem. Commun.*, 2019, **55**, 4627-4630.
19. C. Zhang, S. Liu, T. Chen, Z. Li and J. Hao, *Chem. Commun.*, 2019, **55**, 7370-7373.
20. Y. Chen, R. Guo, X. Peng, X. Wang, X. Liu, J. Ren, J. He, L. Zhuo, J. Sun, Y. Liu, Y. Wu and J. Luo, *ACS Nano*, 2020, **14**, 6938-6946.
21. L. Zhang, G. Fan, W. Xu, M. Yu, L. Wang, Z. Yan and F. Cheng, *Chem. Commun.*, 2020, **56**, 11957-11960.
22. X. Wang, W. Wang, M. Qiao, G. Wu, W. Chen, T. Yuan, Q. Xu, M. Chen, Y. Zhang, X. Wang, J. Wang, J. Ge, X. Hong, Y. Li, Y. Wu and Y. Li, *Sci. Bull.*, 2018, **63**, 1246-1253.
23. P. Wang, Y. Ji, Q. Shao, Y. Li and X. Huang, *Sci. Bull.*, 2020, **65**, 350-358.
24. H. Tao, C. Choi, L. X. Ding, Z. Jiang, Z. Han, M. Jia, Q. Fan, Y. Gao, H. Wang, A. W. Robertson, S. Hong, Y. Jung, S. Liu and Z. Sun, *Chem*, 2019, **5**, 204-214.

25. L. Han, X. Liu, J. Chen, R. Lin, H. Liu, F. Lü, S. Bak, Z. Liang, S. Zhao, E. Stavitski, J. Luo, R. R. Adzic and H. L. Xin, *Angew. Chem., Int. Ed.*, 2019, **58**, 2321-2325.
26. F. Lü, S. Zhao, R. Guo, J. He, X. Peng, H. Bao, J. Fu, L. Han, G. Qi, J. Luo, X. Tang and X. Liu, *Nano Energy*, 2019, **61**, 420-427.
27. Y.-C. Hao, Y. Guo, L.-W. Chen, M. Shu, X.-Y. Wang, T.-A. Bu, W.-Y. Gao, N. Zhang, X. Su, X. Feng, J.-W. Zhou, B. Wang, C.-W. Hu, A.-X. Yin, R. Si, Y.-W. Zhang and C.-H. Yan, *Nat. Catal.*, 2019, **2**, 448-456.
28. L. Zhang, L.-X. Ding, G.-F. Chen, X. Yang and H. Wang, *Angew. Chem., Int. Ed.*, 2019, **58**, 2612-2616.
29. X. Yang, J. Nash, J. Anibal, M. Dunwell, S. Kattel, E. Stavitski, K. Attenkofer, J. G. Chen, Y. Yan and B. Xu, *J. Am. Chem. Soc.*, 2018, **140**, 13387-13391.
30. J. Zhao, X. Ren, X. Li, D. Fan, X. Sun, H. Ma, Q. Wei and D. Wu, *Nanoscale*, 2019, **11**, 4231-4235.
31. C. Lv, Y. Qian, C. Yan, Y. Ding, Y. Liu, G. Chen and G. Yu, *Angew. Chem., Int. Ed.*, 2018, **57**, 10246-10250.
32. W. Qiu, X.-Y. Xie, J. Qiu, W. H. Fang, R. Liang, X. Ren, X. Ji, G. Cui, A. M. Asiri, G. Cui, B. Tang and X. Sun, *Nat. Commun.*, 2018, **9**, 3485.
33. G. Yu, H. Guo, W. Kong, T. Wang, Y. Luo, X. Shi, Abdullah M. Asiri, T. Li and X. Sun, *J. Mater. Chem. A*, 2019, **7**, 19657-19661.
34. T. Xu, D. Ma, T. Li, L. Yue, Y. Luo, S. Lu, X. Shi, A. M. Asiri, C. Yang and X. Sun, *Chem. Commun.*, 2020, **56**, 14031-14034.
35. L. Zhang, X. Ji, X. Ren, Y. Ma, X. Shi, Z. Tian, A. M. Asiri, L. Chen, B. Tang and X. Sun, *Adv. Mater.*, 2018, **30**, 1800191.
36. P. Chen, N. Zhang, S. Wang, T. Zhou, Y. Tong, C. Ao, W. Yan, L. Zhang, W. Chu, C. Wu and Y. Xie, *Pnas* 2019, **116**, 6635-6640.
37. Q. Li, Y. Cheng, X. Li, Y. Guo and K. Chu, *Chem. Commun.*, 2020, **56**, 13009-13012.
38. P. Li, Z. Liu, T. Wu, Y. Zhang, L. Wang, L. Wang, L. Ji, Y. Zhang, Y. Luo, T. Wang, S. Liu, Y. Wu, M. Liu and X. Sun, *J. Mater. Chem. A*, 2019, **7**, 17761-17765.
39. F. Pang, Z. Wang, K. Zhang, J. He, W. Zhang, C. Guo and Y. Ding, *Nano Energy*, 2019, **58**, 834-841.
40. L. Zhao, X. Liu, S. Zhang, J. Zhao, X. Xu, Y. Du, X. Sun, N. Zhang, Y. Zhang, X. Ren and Q. Wei, *J. Mater. Chem. A*, 2021, **9**, 259-263.
41. R. D. Kumar, Z. Wang, C. Li, A. V. Narendra Kumar, H. Xue, Y. Xu, X. Li, L. Wang and H. Wang, *J. Mater. Chem. A*, 2019, **7**, 3190-3196.
42. Z. Fang, P. Wu, Y. Qian and G. Yu, *Angew. Chem., Int. Ed.*, 2020, **59**, 2-9.
43. Y. Liu, Y. Su, X. Quan, X. Fan, S. Chen, H. Yu, H. Zhao, Y. Zhang and J. Zhao, *ACS Catal.*, 2018, **8**, 1186-1191.
44. C. Zhao, S. Zhang, M. Han, X. Zhang, Y. Liu, W. Li, C. Chen, G. Wang, H. Zhang and H. Zhao, *ACS Energy Lett.*, 2019, **4**, 377-383.
45. W. Li, T. Wu, S. Zhang, Y. Liu, C. Zhao, G. Liu, G. Wang, H. Zhang and H. Zhao, *Chem. Commun.*, 2018, **54**, 11188-11191.



46. J. Zhao, J. Yang, L. Ji, H. Wang, H. Chen, Z. Niu, Q. Liu, T. Li, G. Cui and X. Sun, *Chem. Commun.*, 2019, **55**, 4266-4269.
47. Y. Wang, X. Cui, J. Zhao, G. Jia, L. Gu, Q. Zhang, L. Meng, Z. Shi, L. Zheng, C. Wang, Z. Zhang and W. Zheng, *ACS Catal.* 2019, **9**, 336-344.
48. X. Yu, P. Han, Z. Wei, L. Huang, Z. Gu, S. Peng, J. Ma and G. Zheng, *Joule*, 2018, **2**, 1610-1622.
49. C. Chen, D. Yan, Y. Wang, Y. Zhou, Y. Zou, Y. Li and S. Wang, *Small Methods*, 2019, **15**, 1805029.
50. X. Yang, F. Ling, X. Zi, Y. Wang, H. Zhang, H. Zhang, M. Zhou, Z. Guo and Y. Wang, *small*, 2020, **16**, 2000421.
51. S. Zhang, M. Jin, T. Shi, M. Han, Q. Sun, Y. Lin, Z. Ding, L. R. Zheng, G. Wang, Y. Zhang, H. Zhang and H. Zhao, *Angew. Chem., Int. Ed.*, 2020, **59**, 13423-13429.
52. B. H. R. Suryanto, H.-L. Du, D. Wang, J. Chen, A. N. Simonov and D. R. MacFarlane, *Nat. Catal.*, 2019, **2**, 290-296.
53. J. Choi, B. H. R. Suryanto, D. Wang, H.-L. Du, R. Y. Hodgetts, F. M. Ferrero Vallana, D. R. MacFarlane and A. N. Simonov, *Nat. Commun.*, 2020, **11**, 5546.
54. L. Ma, Y. Cheng, G. Cavataio, R. W. McCabe, L. Fu and J. Li, *Appl. Catal. B: Environ.*, 2014, **156-157**, 428-437.
55. L. Ma, Y. Cheng, G. Cavataio, R. W. McCabe, L. Fu and J. Li, *Chem. Eng. J.*, 2013, **225**, 323-330.
56. Q. Ye, L. Wang and R. T. Yang, *Appl. Catal. A: Gen.*, 2012, **427-428**, 24-34.